DR. MICHAEL J ASPINWALL (Orcid ID : 0000-0003-0199-2972)

Article type : Primary Research Article

Temperature acclimation of leaf respiration differs between marsh and mangrove vegetation in a coastal wetland ecotone

Running title: leaf respiration in a marsh-mangrove ecotone

Matthew A. Sturchio[1†], Jeff Chieppa[1,2], Samantha K. Chapman[3], Gabriela Canas[1], Michael J. Aspinwall[1,2*]

[1]*University of North Florida, Department of Biology, Jacksonville, Florida, 32224 USA*

[2]*School of Forestry and Wildlife Sciences, Auburn University, Auburn, Alabama, 36849 USA*

[3]*Department of Biology and Center for Biodiversity and Ecosystem Stewardship, Villanova University, Villanova, Pennsylvania, 19085 USA*

[†]*Present address: Department of Biology and Graduate Degree Program in Ecology, Colorado State University, Fort Collins, CO 80523, USA*

*Corresponding author, phone: +1-(334)-844-8030, email: aspinwall@auburn.edu

Michael J. Aspinwall https://orcid.org/0000-0003-0199-2972

Jeff Chieppa https://orcid.org/0000-0003-2854-1514

Abstract

Temperature acclimation of leaf respiration (R) is an important determinant of ecosystem responses to temperature and the magnitude of temperature-CO_2 feedbacks as climate warms. Yet, the extent to which temperature acclimation of R exhibits a common pattern across different growth conditions, ecosystems, and plant functional types remains unclear. Here, we measured the short-term temperature response of R at six timepoints over a 10-month period in two coastal wetland species (*Avicennia germinans* (C_3 mangrove), *Spartina alterniflora* (C_4 marsh grass)) growing under ambient and experimentally warmed temperatures at two sites in a marsh-mangrove ecotone. Leaf nitrogen (N) was determined on a subsample of leaves to explore potential coupling of R and N. We hypothesized that both species would reduce R at 25 °C (R^{25}) and the short-term temperature sensitivity of R (Q_{10}) as air temperature (T_{air}) increased across seasons, but the decline would be stronger in *Avicennia* than *Spartina*. For each species, we hypothesized that seasonal temperature acclimation of R would be equivalent in plants grown under ambient and warmed temperatures, demonstrating convergent acclimation. Surprisingly, *Avicennia* generally increased R^{25} with increasing growth temperature, although the Q_{10} declined as seasonal temperatures increased and did so consistently across sites and treatments. Weak temperature acclimation resulted in reduced homeostasis of R in *Avicennia*. *Spartina* reduced R^{25} and the Q_{10} as seasonal temperatures increased. In *Spartina*, seasonal temperature acclimation was largely consistent across sites and treatments resulting in greater respiratory homeostasis. We conclude that co-occurring coastal wetland species may show contrasting patterns of respiratory temperature acclimation. Nonetheless, leaf N scaled positively with R^{25} in both species highlighting the importance of leaf N in predicting respiratory capacity across a range of

growth temperatures. Patterns of respiratory temperature acclimation shown here may improve predictions of temperature controls of CO_2 fluxes in coastal wetlands.

Keywords: coastal wetlands, coordination theory, *Avicennia germinans*, homeostasis, respiratory capacity, *Spartina alterniflora*, thermal acclimation

Introduction

Roughly half of terrestrial gross primary production (GPP) is returned to the atmosphere each year via autotrophic respiration (Piao et al., 2013), and approximately half of plant respiration comes from leaves (Atkin et al., 2007; Atkin et al., 2015). As a result, leaf respiration (*R*, typically measured in darkness as CO_2 efflux) is an important parameter for simulating carbon (C) cycling in terrestrial biosphere models (TBMs) and associated earth system models (Fisher et al., 2014; Atkin et al., 2015). Leaf *R* is determined by a series of enzymatic reactions in the cytosol and mitochondria and is therefore temperature dependent. In the short-term (minutes, hours), *R* increases quasi-exponentially with increasing measurement temperature before reaching an optimum (typically between 50 and 60 °C; O'Sullivan et al., 2017; Aspinwall et al., 2017). This temperature sensitivity has led to the prediction that climate warming will accelerate the positive feedback between CO_2 and temperature. However, there is considerable evidence that plants may 'acclimate' to seasonal or spatial variation in growth temperature by modifying the short-term temperature response of *R*. Many plants acclimate to increasing growth temperatures (increasing seasonal temperatures, experimental warming) by reducing *R* at a set measurement temperature (i.e. 25 °C, Slot & Kitajima, 2015). This type of acclimation is referred to as Type II acclimation and is considered a change in respiratory capacity (Atkin & Tjoelker, 2003). Less commonly, plants respond to increasing growth temperatures by reducing the short-term temperature sensitivity of *R* (Q_{10}, activation energy, Slot & Kitajima, 2015). This type of acclimation is referred to as Type I acclimation (Atkin & Tjoelker, 2003). Both Type II and Type I temperature acclimation of *R* result in varying degrees of respiratory homeostasis across a range of prevailing growth temperatures (Slot & Kitajima, 2015). At larger scales, the reduced sensitivity of *R* to temperature (i.e. greater homeostasis) should reduce the positive feedback between temperature and CO_2 as climate warms (King et al., 2006; Smith & Dukes,

2013). Moreover, when TBMs account for temperature acclimation of leaf CO_2 exchange, higher net C storage is predicted under climate warming than would be predicted without temperature acclimation (Lombardozzi et al., 2015; Smith et al., 2016).

Although leaf *R* and patterns and mechanisms of respiratory temperature acclimation are better understood and increasingly represented in TBMs, important knowledge gaps and data uncertainties remain. One uncertainty is whether temperature acclimation of leaf *R* is consistent over time (i.e. seasons), across spatially separated sites, and across plants growing under current and warmed climates. Most evidence for temperature acclimation of leaf *R* comes from three types of studies: field studies of plants responding to seasonal variation in temperature at individual sites (Atkin et al., 2000; Lee et al., 2005; Ow et al., 2008, 2010; Tjoelker et al., 2008; 2009), field studies that implement warming overtop natural seasonal temperature changes (Bruhn et al., 2007; Aspinwall et al., 2016), and warming studies conducted under controlled conditions on small plants, usually for short time periods (Bolstad et al., 2003; Cheesman & Winter, 2013; Drake et al., 2015). Acclimation responses observed across all studies could be the result of a common mechanism. Indeed, two experiments with tree species from warm-temperate and boreal climates showed that seasonal temperature acclimation of *R* was equivalent between trees grown under ambient and experimentally warmed temperatures, indicating convergent acclimation (Aspinwall et al., 2016; Reich et al., 2016). Thus, physiological responses to climate warming might be predicted from studies of physiological responses to seasonal temperature changes. There is also evidence that temperature acclimation-over-time and temperature acclimation-across-space may result in similar changes in leaf *R* (Vanderwel et al., 2015). However, additional experiments are required to determine whether plants show convergent patterns of temperature acclimation of leaf *R* over seasons, sites, and with climate warming. This will help determine whether temperature acclimation responses are common and generalizable across a wide range of environmental conditions.

Whether temperature acclimation of leaf physiology differs between C_3 and C_4 plants is also an important uncertainty. It has been hypothesized that C_4 plants may show limited capacity for temperature acclimation due to a more complex physiology (Yamori et al., 2014). Support for this hypothesis is mixed. Yamori et al., (2014) synthesized results from individual studies with different methodologies and growth temperatures and found that C_3 plants generally showed greater ability for photosynthetic temperature acclimation than C_4 plants. However, Smith &

Dukes, (2017) grew several C_3 and C_4 species together in a controlled environment under similar temperature treatments and found that C_3 and C_4 plants showed comparable temperature acclimation of photosynthesis and leaf *R* (Smith & Dukes, 2017). Additional studies that compare temperature acclimation of C_3 and C_4 species will help clarify whether predictions of temperature acclimation responses need to be photosynthetic-type specific.

Leaf *R* and temperature acclimation of leaf *R* also remain understudied in some regions and ecosystems, including coastal wetlands. These ecosystems are typically dominated by C_4 marsh grass species and C_3 mangrove species. Despite covering a small proportion of the earth's surface, coastal marsh and mangrove ecosystems play an important role in global C cycling (Lugo & Snedeker 1974; Bouillon et al., 2008; Donato et al., 2011; Mcleod et al., 2011; Lu et al., 2017). These ecosystems have high rates of C accumulation and burial, slow decomposition rates, and a relatively high fraction of biomass belowground. Autotrophic *R* (a large proportion of which is leaf *R*) is a major component of the coastal wetland C cycle, accounting for an estimated ~50% of GPP in marsh and mangrove ecosystems (Alongi, 2020). However, direct measures of leaf *R* or its temperature sensitivity over space and time are relatively rare for marsh and mangrove species. Only a handful of studies have quantified temperature acclimation of leaf *R* in mangrove species (see Akaji et al., 2019; Aspinwall et al., 2021) and none have examined temperature acclimation in marsh grasses. As a result, the extent to which temperature acclimation of *R* leads towards homeostasis of realized (*in situ*) *R* over space and time in coastal wetland plants remains unclear.

Studies that examine patterns of temperature acclimation of leaf *R* over space and time may provide insight into spatial and temporal variability in photosynthetic capacity. Respiration plays an important role in several processes that influence photosynthesis including nitrate reduction, phloem loading, and turnover of phospholipid membranes and proteins. Rubisco accounts for a large fraction of leaf protein in C_3 plants (Evans 1989; Hikosaka & Shigeno 2009; Aspinwall et al., 2019) and respiratory-driven turnover of Rubisco is important for maintaining photosynthetic capacity under natural conditions. This likely explains why leaf *R* and maximum rates of Rubisco carboxylation (V_{cmax}) (both measured at 25 °C) are positively related across a wide range of C_3 species (Wright et al., 2004; Atkin et al., 2015; O'Leary et al., 2019). Recent analyses also support the theory that temperature acclimation of leaf *R* helps maintain 'optimal' photosynthetic capacity in C_3 species (Wang et al., 2020). Leaf *R* data are limited for C_4 species

(Atkin et al., 2015) such that broadscale photosynthesis – respiration relationships are unclear across C_4 species, although similar coupling of *R* and photosynthesis is expected.

Coupling of photosynthetic and respiratory capacity may be related to total leaf N which represents total photosynthetic and respiratory enzyme content. Indeed, across C_3 species, leaf N scales positively with both V_{cmax} and *R* at 25 °C (Reich et al., 2008; Walker et al., 2014; Atkin et al., 2015). In C_4 species, positive relationships between leaf N and net photosynthesis have also been observed (Ghannoum et al., 2005), although leaf N – leaf *R* relationships have not been widely explored. Similar coupling of leaf N, V_{cmax}, and *R* across changing growth temperatures is sometimes observed within C_3 species growing at individual sites (Tjoelker et al., 1999; Lee et al., 2005; Crous et al., 2017). Thus, changes in leaf N may also partly explain coordinated temperature acclimation of leaf *R* and photosynthetic capacity (Wang et al., 2020). For these reasons, many land surface models predict functional-type specific rates of *R* using either leaf N on an area or mass-basis or estimates of V_{cmax} at 25 °C (Fisher et al., 2014; Lawrence et al., 2019).

In this study we repeatedly measured the short-term temperature responses of leaf *R* over a 10-month period in a C_3 mangrove species (*Avicennia germinans*) and C_4 marsh grass species (*Spartina alterniflora*) grown *in situ* under ambient temperatures and experimental warming at two spatially separated sites in a marsh-mangrove ecotone on the Atlantic coast of Florida (USA). The ecotone represents a transitional zone where the southern part of temperate saltmarsh habitat converges with the northern limit of tropical mangrove habitat. From each short-term temperature response measurement, we estimated *R* at 25 °C (R^{25}) and the short-term temperature sensitivity of leaf *R* (Q_{10}). We also used individual short-term temperature response measurements to estimate realized (*in situ*) *R* at prevailing air temperatures. We determined leaf N on a subset of leaves collected at both sites, in both treatments, on different measurement dates. For each species, we hypothesized that R^{25} and the short-term Q_{10} of *R* would decrease with experimental warming and as seasonal air temperatures increased. Importantly, we expected that the decline in R^{25} and the short-term Q_{10} of *R* with increasing seasonal temperatures would be equivalent in plants growing under ambient and warmed temperatures at both sites, demonstrating convergent temperature acclimation of *R*. However, given that C_4 species may show lower capacity for temperature acclimation than C_3 species (Yamori et al., 2014), we hypothesized that acclimation responses would be greater in *Avicennia* than *Spartina*. In turn, we

expected greater homeostasis of realized *R* across a range of prevailing growth temperatures in *Avicennia* than *Spartina*. Finally, for each species, we hypothesized that leaf N concentrations would scale positively with R^{25} over time and across sites and treatments, providing an explanation for convergent temperature acclimation of *R*.

Materials and methods

Study sites and experimental design

This study took place at two sites in the Guana Tolomato Matanzas National Estuarine Research Reserve (GTMNERR) on the Atlantic coast of Florida, near St. Augustine. The estuarine vegetation in GTMNERR represents a marsh-mangrove ecotone. The southern part of saltmarsh habitat converges and overlaps with the northern limit of mangrove habitat in Florida, although mangroves are increasingly common north of GTMNERR (Dix et al., 2021). The north site (NS) was located roughly 14 km north of St. Augustine along the Tolomato River near the northern edge of GTMNERR (30°00'41.9"N 81°20'39.2"W). The south site (SS) was located roughly 20 km south of St. Augustine (34 km to the south of NS) and just north of the Matanzas Inlet (29°43'38.3"N 81°14'25.0"W). NS and SS have similar elevations, and average annual precipitation at the GTMNERR reserve is 1317 mm (Chapman et al., 2021). Mean annual temperature (2001–2018) at St. Augustine is 20.8 °C. The highest monthly mean daily max temperature (July) is 32.0 °C, and the lowest monthly mean daily low temperature (January) is 11.1 °C (NOAA-NCDC). *Spartina alterniflora* (smooth cordgrass) and *Avicennia germinans* (black mangrove) are common at both sites although *Avicennia* trees are generally larger and more abundant at SS. *Spartina* is a C_4 grass (PEP-CK subtype) that dominates temperate estuaries along the east coast of North America and warm-temperate estuaries in the Gulf of Mexico and northern Florida (Lugo et al., 1999). *Avicennia* is a broadly distributed mangrove species native to warm-temperate, subtropical, and tropical regions of the Americas and Africa. On the Atlantic coast, its distribution stretches from North Florida to southern Brazil. All mangroves selected for this study ranged from 4-11 years old in 2018 with an average age of 7.4 years and 7.2 years at SS and NS respectively (Chapman et al., 2021).

The study included six replicates of four treatment plots at each site. The four treatments were: *Avicennia* ambient, *Avicennia* warmed, *Spartina* ambient, and *Spartina* warmed (Chapman et al., 2021). Treatment plots were randomly positioned within a one-hectare area at each site. The warmed plots were enclosed in 1.5m × 1.5m × 1.5m chambers, framed with PVC and wrapped in 6 mil polyethylene greenhouse film (Greenhouse Megastore, Danville, IL, USA) that transmits ~90% of photosynthetically active radiation. The chamber top was left open to allow for air circulation (mixing) and natural rainfall. The chambers 'trap' radiation causing the chamber air to passively warm. Consequently, only daytime warming is achieved using this design with minimal warming occurring during cloudy weather, when radiation is limited, or at night. However, unlike infrared heaters, chambers warm air temperatures rather than canopy surface temperatures (e.g. De Boeck et al., 2012; Smith et al., 2020) and do not inhibit dew formation (Feng et al., 2021). In the event of a tropical storm, we removed the polyethylene film from the PVC frames so that chambers would not become airborne. At each site, air temperature (T_{air}) and relative humidity (RH) were measured every 30 minutes in the center of two ambient and warmed treatment plots per species using an air temperature/RH sensor covered in a solar radiation shield (HOBO MX2302 External Temperature/RH Sensor, Onset Computer Corp., Bourne, MA).

Daily maximum, mean, and minimum T_{air}, RH, and vapor pressure deficit at both sites and treatments (averaged across species) are shown in Fig. S1. Averaged over time, mean daily T_{air} was 0.63 °C and 0.66 °C higher in warmed plots than in the ambient plots at NS and SS (Fig. S2a,c), respectively (NS ambient mean daily T_{air} = 22.8 ± 5.1 (standard deviation) °C, NS warmed mean daily T_{air} = 23.5 ± 5.3; SS ambient mean daily T_{air} = 22.9 ± 5.1 °C, SS warmed mean daily T_{air} = 23.6 ± 5.4 °C). Daily maximum T_{air} was on average 3.1 °C and 3.2 °C higher in the warmed plots than the ambient plots at NS and SS (Fig. S2b,d), respectively (NS ambient daily max T_{air} = 28.1 ± 5.2 ± °C, NS warmed mean daily T_{air} = 31.2 ± 5.8 °C; SS ambient daily max T_{air} = 27.5 ± 5.2 °C, SS warmed daily max T_{air} = 30.7 ± 5.8 °C). Warming of this magnitude (1-3 °C) is expected by 2050 throughout the southeast U.S. (Ashfaq et al., 2016). Daily mean RH was similar between treatments and sites and averaged 83.1 ± 7.1% and 85.3 ± 8.4% at NS and SS, respectively (Fig. S1b,e). Daily mean VPD was generally <1 at both sites, with only small differences in VPD between warmed and ambient treatment plots (Fig. S1c,f).

246 ***Temperature response of leaf respiration***

247 Measurements of the short-term temperature response of leaf dark respiration (*R*) were
248 conducted at six timepoints (October, December, February, April, June, July) over a 10-month
249 period. Each measurement campaign was split over a maximum of two days at each site (four
250 days total). On each measurement day we collected two entire recent and fully developed upper
251 canopy leaves from each *Spartina* plot and three recent and fully developed upper canopy leaves
252 from each *Avicennia* plot. *Spartina* leaves were excised ~2 cm distal to the ligule. Leaves were
253 collected pre-dawn (04:30 – 06:00 local time) to avoid activation of photosynthesis. The excised
254 leaves were placed in Ziplock bags with moist paper and transferred to the lab in complete
255 darkness. Previous studies have found no effect of leaf removal on *R* measurements (O'Sullivan
256 et al., 2013; Aspinwall et al., 2017; 2019). All measurements were completed the same day as
257 leaf collection. We found no evidence that *R* changed with time since leaf removal; rates of *R* at
258 20 °C did not vary with time of day in either species. Leaf area (cm^2) of the measured leaves was
259 determined with a leaf area meter (LI-3000C, LI-COR BioSciences, Lincoln, NE, USA) just
260 prior to measurements of *R*. Leaf area data were used to calculate *R* per unit area (R_{area} μmol m^{-2}
261 s^{-1}).

262 Short-term temperature response curves of *R* were completed by sealing all excised
263 leaves inside a large gas-exchange chamber (3010-GWK1, Heinz Walz GmbH, Effeltrich,
264 Germany) connected to a portable infrared gas-analyzer (LI-6400XT, LiCor Inc, Lincoln, NE,
265 USA). The large gas-exchange chamber was set at 20 °C, while the flow rate and reference CO_2
266 (controlled by the infrared gas-analyzer) were set at 500 mol s^{-1} and 410 μmol mol^{-1},
267 respectively. T_{leaf} on the abaxial surface of the leaf was continuously measured with a small-
268 gauge copper constantan thermocouple wire attached to a LI-6400XT external thermocouple
269 adaptor (LI6400–13). To facilitate measurements of *R*, the airflow from the chamber was
270 connected to the 'sample' gas line of the LI-6400XT fitted with an empty and closed 2×3 cm
271 cuvette. The incoming air was dried before entering the 3010-GWK1 chamber by routing the
272 incoming air through the LI-6400XT desiccant column. Once rates of *R* reached steady-state at
273 20 °C (~5 min) the chamber temperature was increased from 20 °C – 40 °C at a rate of 1°C per
274 minute using the chamber software (GFS-Win, Heinz Walz GmbH) while continuously (30
275 second interval) measuring R_{area} and T_{leaf}. Each short-term temperature response measurement
276 took approximately 25 minutes to complete. After temperature response measurements were

completed, leaves were dried at 70 °C for ~72 hours after which leaf dry mass was determined and leaf dry mass per unit area (LMA, g m^{-2}) was calculated. Leaf *R* per unit mass (R_{mass}, nmol g^{-1} s^{-1}) was calculated by dividing R_{area} (×1000) by LMA. All individual short-term temperature response curves of R_{area} and R_{mass} are shown in Fig.s S3 and S4. Each individual measurement leaf was ground into a fine powder with a ball mill and dried at 105 °C for ~16 hours, stored under desiccation, and leaf N per unit mass (N_{mass}, % or g N kg^{-1}) was determined using a combustion elemental analyzer (Rapid MAX N, Elementar Americas Inc., Ronkonkoma, NY, USA). Leaf N per unit area (N_{area}, g N m^{-2}) was calculated as the product of %N and LMA.

Modelling the temperature response of respiration

Nonlinear regression was used to model the temperature response of leaf *R* (area- and mass-basis). Nonlinear models were fit using Rstudio (R v.3.6.1, Rstudio v.1.2.1335; R Core Team, 2013). We compared the suitability of three algorithms: (1) a polynomial function, which describes the non-linear relationship between *ln*-transformed *R* and T_{leaf} (Heskel et al., 2016; Patterson et al., 2018), (2) an exponential function with a single Q_{10} value (Ryan, 1991), and (3) a modified Arrhenius function (Lloyd & Taylor, 1994). The polynomial function is written as:

(1) $ln\ R = a + bT + cT^2$ or

(2) $R = e^{a + bT + cT^2}$

where *T* is T_{leaf} and *a* is an estimate of *ln R* at 0 °C, *b* is the slope of temperature response of *ln R* at 0 °C, and *c* describes any nonlinearity in the temperature response of *ln R* with increasing T_{leaf}. The differential of Eqn 2 can be used to estimate the Q_{10} of *R* at any T_{leaf}:

(3) $Q_{10} = e^{10 \times (b + 2cT)}$

The polynomial function (Equation 1) provided the best fit to our data (all $R^2 > 0.98$, all $p < 0.0001$), with a strong linear relationship between observed and predicted values of *ln R* ($R^2 = 0.998$), and residual values normally distributed around zero with little pattern associated with increasing T_{leaf}. Thus, we used the polynomial equation to model the temperature response of *R* and used coefficients *a*, *b* and *c* to estimate R_{area} and R_{mass} at 25 °C (R_{area}^{25}, R_{mass}^{25}), and the Q_{10} of

306 R at 25 °C (Q_{10}^{25}) for each leaf. Mean (± standard error) values of a, b, and c for each species,
307 timepoint, site, and treatment are provided in Tables S1 and S2.
308 To determine how seasonal changes in the short-term temperature response of R (i.e.
309 seasonal temperature acclimation) influenced realized rates of R in both species, we used
310 parameters a, b, and c (Equation 1&2) from individual temperature response curves to estimate
311 realized (*in situ*) R (area- and mass-basis) at the prevailing mean daily T_{air} when sampling took
312 place. We separated the data by species, site, and treatment and determined the long-term
313 temperature sensitivity of realized R using an exponential function (Ryan, 1991) that estimates
314 the Q_{10} of R (constant across the measurement temperature range) and R at a reference
315 temperature of 18 °C (R_{18}) which is near the lowest mean daily T_{air} across sites and treatments.
316 For each species, we compared Q_{10} and R_{18} estimates between sites and treatments by calculating
317 95% confidence intervals (standard error × 1.96). When confidence intervals for Q_{10} and R_{18} did
318 not overlap between sites or treatments, we fit separate temperature response functions for each
319 site or treatment. If confidence intervals overlapped, suggesting that parameters were not
320 different between sites or treatments, we fit a single temperature response function across all
321 data.
322 We also quantified the degree of respiratory homeostasis *across seasons* by calculating a
323 temperature acclimation ratio for each measurement date following Slot & Kitajima, (2015):
324 $Acclim_{homeo}$ = R at lowest mean daily T_{air} / R at mean daily T_{air}. The numerator is individual
325 estimates of *in situ* R at the coolest timepoint (i.e. lowest mean daily T_{air}; held constant), and the
326 denominator is individual estimates of *in situ* R, for the same treatment plot, estimated at each
327 timepoint warmer than the coolest timepoint. Ratios were calculated separately for each species,
328 site, and treatment. Ratios > 1 indicate temperature acclimation resulting in 'overcompensation',
329 ratios = 1 indicate temperature acclimation resulting in complete homeostasis, and ratios < 1
330 indicate temperature acclimation resulting in partial homeostasis (Slot & Kitajima, 2015). Ratios
331 were plotted against the change in prevailing mean daily T_{air} across seasons to assess changes
332 respiratory homeostasis with increasing seasonal temperatures.
333
334 ***Data analysis***
335 All analyses were performed using Rstudio (R v.3.6.1, Rstudio v.1.2.1335; R Core Team, 2013).
336 As a preliminary step, we carried out variance partitioning to determine the proportion of the

overall variance in each trait (e.g. R_{area}^{25}) explained by different experimental factors (species, measurement dates, site, treatment). The variance partitioning results indicated that 'species' accounted for most of the trait variance (16-68%), while other factors generally explained a much smaller proportion of the variance (0-7%) (Fig. S5). Therefore, the remainder of the analysis was conducted separately for each species.

For each species, we used analysis of variance (ANOVA) to test the effects of measurement date (i.e. time), temperature treatment (ambient, warmed), site (NS, SS) and their respective interactions on R_{area}^{25}, R_{mass}^{25}, Q_{10}^{25}, LMA, N_{mass}, and N_{area}. For consistency, we analyzed predicted values of R_{area}^{25} and R_{mass}^{25} derived from our temperature response models rather than observed values at 25 °C, although predicted and observed values were nearly identical given the high resolution of our temperature response data. Homogeneity of variance for model results were tested using Levene's and Shapiro-Wilk tests. Data were log or square-root transformed as necessary.

For each species, analysis of covariance (ANCOVA) was used to test relationships between R_{area}^{25}, R_{mass}^{25}, Q_{10}^{25}, LMA, N_{mass}, and N_{area} values and mean daily T_{air} of the preceding 7 days and determine whether relationships differed between sites or treatments. If seasonal temperature acclimation of leaf R occurred, we expected negative linear relationships between mean daily T_{air} and R_{area}^{25}, R_{mass}^{25}, or Q_{10}^{25}. The strength of acclimation is indicated by the slope of this relationship; a more negative slope estimate indicates stronger acclimation. In this model, site and treatment were treated as factors and mean daily T_{air} a covariate. A significant (P<0.05) interaction between mean daily T_{air} and site or treatment indicated that site or treatment affected the relationship between mean daily T_{air} and the response variable (e.g. R_{area}^{25}), and different slope parameters were required for each site or treatment. If site, treatment, and mean daily T_{air} were significant (P<0.10), with no interactions, equations with different intercepts for each site or treatment, but a common slope, were fit to the data. If only mean daily T_{air} was significant, one equation describing the relationship between mean daily T_{air} and the response variable was fit to data from both sites and treatments. ANCOVA was also used to test whether leaf N (N_{mass}, N_{area}) scales positively with respiratory capacity (R_{area}^{25}, R_{mass}^{25}), and whether site or treatment changes the relationship between leaf N and respiratory capacity. In addition, ANCOVA was used to test relationships between $Acclim_{homeo}$ (measure of respiratory homeostasis) and the change in mean daily T_{air} over time, and potential modifying effects of site or treatment.

Results

Leaf R, leaf N, and LMA over time, sites, and temperature treatments

In *Avicennia*, R_{area}^{25}, R_{mass}^{25}, and N_{area} varied over time, but temporal differences in these traits depended upon site (significant date × site interactions Table 1). R_{area}^{25} was higher at NS than SS in December 2019 (NS: 1.09 ± 0.04 μmol m^{-2} s^{-1}, SS: 0.86 ± 0.04 μmol m^{-2} s^{-1}), but lower at NS than SS in July 2020 (NS: 1.05 ± 0.04 μmol m^{-2} s^{-1}, SS: 1.30 ± 0.04 μmol m^{-2} s^{-1}, Fig. 1a). R_{mass}^{25} was also lower at NS than SS in July 2020 (NS: 4.36 ± 0.36 nmol g^{-1} s^{-1}, SS: 7.64 ± 0.36 nmol g^{-1} s^{-1}, Fig. 1c). N_{area} was higher at NS (4.29 ± 0.17 g N m^{-2}) than SS (3.22 ± 0.23 g N m^{-2}) in October 2019 (Fig. 1i). R_{area}^{25}, R_{mass}^{25}, and N_{area} were similar between sites at the remaining timepoints.

Across both sites, warming increased *Avicennia* R_{area}^{25} by 8% (ambient R_{area}^{25} = 1.05 ± 0.02 μmol m^{-2} s^{-1}, warmed R_{area}^{25} = 1.14 ± 0.02 μmol m^{-2} s^{-1}). However, warming effects on R_{mass}^{25} differed between sites (treatment × site interaction, Table 1). Warming did not affect R_{mass}^{25} at NS (mean = 4.43 ± 0.21 nmol g^{-1} s^{-1}) but increased R_{mass}^{25} by 24% at SS (ambient R_{mass}^{25} = 4.56 ± 0.22 nmol g^{-1} s^{-1}, warmed R_{mass}^{25} = 5.67 ± 0.23 nmol g^{-1} s^{-1}).

In *Avicennia*, Q_{10}^{25} varied over time (Table 1) and was highest in February and April 2020 (2.25 ± 0.05 and 2.26 ± 0.05, respectively), and lowest in June 2020 (1.94 ± 0.05, Fig. 1e). Q_{10}^{25} did not differ between treatments but differed between sites (Table 1). Q_{10}^{25} was lower at NS (2.03 ± 0.03) than SS (2.17 ± 0.03). LMA showed a complex pattern; with variation over time depending upon both treatment and site (treatment × date × site, Table 1) (Fig. 2g). LMA was highest in warmed plants at NS in July 2020 (272 ± 10.4 g m^{-2}) and October 2019 (277 ± 10.4 g m^{-2}), and lowest in ambient plants at SS in July 2020 (168 ± 10.4 g m^{-2}). N_{mass} did not differ between sites or treatments (Table 1), but was 15% higher in June 2020 (17.1 ± 0.60 g N kg^{-1}) than February 2020 (14.9 ± 0.60 g N kg^{-1}).

In *Spartina*, R_{area}^{25}, R_{mass}^{25}, and LMA varied over time, but temporal variation in these traits depended upon site (i.e., date × site interaction, Table 1, Fig. 2). Although date × site interactions were significant for R_{area}^{25}, post-hoc analysis revealed that differences between sites occurred on different dates (October 2019, R_{area}^{25} was higher at SS (1.71 ± 0.11 μmol m^{-2} s^{-1}) than at NS in February 2020 (1.19 ± 0.10 μmol m^{-2} s^{-1}) (Fig. 1b)). R_{mass}^{25} was generally higher during winter (December, February) and lower during summer (June, July) (Fig. 1). In December

2019, R_{mass}^{25} was significantly higher at NS (13.6 ± 0.5 nmol g^{-1} s^{-1}) than SS (9.9 ± 0.5 nmol g^{-1} s^{-1}). R_{mass}^{25} was similar between sites across all other dates. LMA showed the opposite seasonal pattern of R_{mass}^{25}; lowest in winter and highest during peak growing season. In February 2020, LMA was significantly lower at NS (99 ± 5.9 g m^{-2}) than SS (128 ± 5.9 g m^{-2}). On average, warming reduced R_{mass}^{25} 6.4% across all timepoints (Table 1, ambient R_{mass}^{25}: 10.9 ± 0.2 nmol g^{-1} s^{-1}, warmed R_{mass}^{25}: 10.2 ± 0.2 nmol g^{-1} s^{-1}) but had no effect on R_{area}^{25} or LMA.

In *Spartina*, Q_{10}^{25} was similar across sites and treatments (Table 1) but varied over time and was higher in February 2020 (1.94 ± 0.03) than June 2020 (1.77 ± 0.03) (Fig. 1e). Temporal variation in N_{mass} depended upon temperature treatment (significant date × treatment interaction, Table 2). In February 2020, N_{mass} was significantly lower in warmed plants (15.7 ± 0.6 g N kg^{-1}) than ambient plants (18.3 ± 0.6 g N kg^{-1}) (Fig. 1k). N_{area} did not differ between dates, treatments, or sites (and no interactions, Table 1) and averaged (2.04 ± 0.08 g N m^{-2}).

Growth temperature – leaf trait relationships

For *Avicennia*, ANCOVA results indicated that the response of R_{area}^{25} and R_{mass}^{25} to mean daily T_{air} differed between sites (T_{air} × site interaction, Table 2). At NS, R_{area}^{25} and R_{mass}^{25} showed no clear relationship with mean daily T_{air} (Fig. 2a,c). At SS, R_{area}^{25} and R_{mass}^{25} both increased with increasing mean daily T_{air} (Fig. 2a,c, Table S3). In agreement with our ANOVA results, we found that warming generally increased R_{area}^{25} and R_{mass}^{25} in *Avicennia* (Fig. 2a,c). These results provide no evidence for temperature acclimation of respiratory capacity (Type II acclimation) in *Avicennia* growing at the species northern range limit. However, Q_{10}^{25} decreased as mean daily T_{air} increased (Table 2, Fig. 2e), indicating Type I temperature acclimation. This acclimation response was consistent across treatments and sites, although the intercept of the relationship was lower at NS than SS (Table 2, Fig. 2e, Table S3).

In *Avicennia*, LMA decreased as mean daily T_{air} increased, but the slope of the relationship differed between sites (T_{air} × site interaction, Table 2, Table S3). LMA decreased faster with increasing T_{air} at SS than NS (Fig. 2g, Table S3). Similar to our ANOVA results, warming effects on LMA differed between sites (treatment × site interaction, Table 2). Warming did not change LMA at NS but reduced LMA at SS. Lastly, N_{mass} increased as mean T_{air} increased and did so consistently across treatments and sites (Table 2, Fig. 2i).

Spartina showed clear evidence of Type II and Type I temperature acclimation of R across seasons, which was consistent across treatments and sites. Specifically, R_{mass}^{25} decreased with increasing mean daily T_{air}; the intercept of the relationship was higher at NS than SS (Table 2, Fig. 2d, Table S3). This relationship accounts for increasing LMA with T_{air} (Fig. 2h). Q_{10}^{25} also decreased with increasing mean daily T_{air} and did so consistently across sites and treatments (Fig. 2f, Table S3). N_{mass} declined with increasing T_{air}, although the decline in N_{mass} with increasing T_{air} differed between treatments (T_{air} × treatment interaction, Table 2, Fig. 2j). Across sites, warming reduced the intercept and slope of the relationship between T_{air} and N_{mass} (Fig. 2j, Table S3). N_{area} showed no relationship with mean daily T_{air} in either species.

Realized temperature response of R and degree of respiratory homeostasis

In *Avicennia*, the realized Q_{10} of R_{area}, which reflects the *long-term* acclimated temperature response of R, differed between sites and was 2.01 ± 0.09 at NS and 3.12 ± 0.24 at SS (Fig. 3a). The realized Q_{10} of R_{mass} also differed between sites and was 2.25 ± 0.15 at NS and 5.14 ± 0.84 at SS (Fig. 3). Realized Q_{10} values did not differ between treatments at either site. These realized Q_{10} values are similar or higher than Q_{10}^{25} estimates (Fig. 1). Thus, weak temperature acclimation of R in *Avicennia* resulted in little dampening of the temperature sensitivity of realized R. Furthermore, the temperature acclimation ratio $Acclim_{homeo}$, which describes the degree of respiratory homeostasis, declined as seasonal temperatures increased indicating a reduction in respiratory homeostasis with larger increases in mean daily T_{air} (Fig. 4a,c). The decline in $Acclim_{homeo}$, calculated using *in situ* estimates of R_{area} and R_{mass}, was consistent across treatments but was more pronounced at SS (R_{area} slope = -0.08, R_{mass} slope = -0.09) than NS (R_{area} slope = -0.05, R_{mass} slope = -0.06; Fig. 4a,c).

In *Spartina*, the realized Q_{10} of R_{area} and R_{mass} was 1.79 ± 0.09 and 1.34 ± 0.05, respectively, and was consistent across sites and treatments (Fig. 3b,d). These realized Q_{10} values are lower (roughly -10% to -30%) than Q_{10}^{25} estimates, reflecting a dampening of the long-term temperature sensitivity of R resulting from both Type II and Type I temperature acclimation. $Acclim_{homeo}$ declined as the change in mean daily T_{air} increased and did so consistently across sites (R_{area} slope = -0.06, R_{mass} slope = -0.03; Fig. 4b,d). When $Acclim_{homeo}$ was calculated using *in situ* estimates of R_{mass}, the decline in $Acclim_{homeo}$ with increasing temperature was lower in *Spartina* than in *Avicennia* (Fig. 4c,d). The intercept of the relationship between $Acclim_{homeo}$ and

460 the change in mean daily T_{air} was higher at NS (R_{area} intercept = 1.17, R_{mass} intercept = 1.09) than
461 SS (R_{area} intercept = 1.06, R_{mass} intercept = 0.97; Fig. 4b,d). We conclude that *Spartina* showed
462 stronger temperature acclimation of *R* and maintained greater homeostasis of realized *R* than
463 *Avicennia*.
464
465 ***Leaf N – R relationships***
466 We found that leaf N scaled positively with respiratory capacity in both species. However, in
467 some cases, relationships between leaf N and respiratory capacity depended upon treatment or
468 site (Table 3). In *Avicennia*, R_{area}^{25} increased with N_{area} at SS but not NS, and R_{area}^{25} at a given
469 N_{area} was higher under warming than ambient conditions (Table 3, Fig. 5a). N_{mass} and R_{mass}^{25}
470 scaled positively although the intercept was lower at NS than SS (Table 3, Fig. 5c, Table S4).
471 Overall, N_{area} explained 25% of the variation in R_{area}^{25}, while N_{mass} explained 53% of the
472 variation in R_{mass}^{25} (Table S4).
473 In *Spartina*, the slope of the $N_{area} - R_{area}^{25}$ relationship was slightly lower at NS than SS
474 (Table 3, Fig. 5b, Table S4). The positive relationship between N_{mass} and R_{mass}^{25} was consistent
475 across treatments and sites (Table 3, Fig. 5d, Table S4). N_{area} explained 74% of the variation in
476 R_{area}^{25}, while N_{mass} explained 51% of the variation in R_{mass}^{25} (Table S4). Although temperature
477 acclimation of *R* differed between *Avicennia* and *Spartina*, changes in leaf N explained
478 temperature acclimation patterns in both species.
479
480 **Discussion**
481 We set out to test whether two contrasting coastal wetland species (*Avicennia germinans*,
482 *Spartina alterniflora*), individually, show patterns of temperature acclimation of leaf *R* that are
483 equivalent across seasons, current and warmed climates, and spatially separated sites. In
484 *Avicennia*, we found that R_{area}^{25} and R_{mass}^{25} showed no relationship with prevailing T_{air} at the
485 north site, increased with T_{air} at the south site, and generally increased with experimental
486 warming across both sites. Thus, *Avicennia* showed no evidence for convergent temperature
487 acclimation of respiratory capacity. Even so, Q_{10}^{25} decreased as seasonal temperatures increased
488 and did so consistently across sites and treatments. In *Spartina*, R_{mass}^{25} and Q_{10}^{25} both declined as
489 seasonal temperatures increased. This pattern of seasonal temperature acclimation was largely
490 consistent across sites and treatments supporting our expectation of convergent temperature

acclimation. However, our results did not support our hypothesis that temperature acclimation of *R* would be weaker in *Spartina* (a C_4 species) than *Avicennia* (a C_3 species). Species differences in temperature acclimation resulted in different degrees of respiratory homeostasis across seasons and treatments, with implications for climate warming impacts on coastal wetland CO_2 fluxes. We conclude that co-occurring species may show contrasting patterns of temperature acclimation. Although temperature acclimation patterns differed between these two dominant coastal wetland plant species, we found that leaf N scaled positively with leaf *R* in both species, providing an explanation for contrasting patterns of respiratory temperature acclimation that may also inform predictions of temporal or spatial variability in leaf *R* in coastal wetlands.

There are several possible explanations for the lack of strong temperature acclimation in *Avicennia*. Coastal wetlands are dynamic systems where water levels (i.e. tides) and salinity vary diurnally and seasonally. Salinity depends on proximity to the ocean and freshwater inputs, seasonality of precipitation, and evaporation rates which change with temperature. In our experiment, the southern site (SS) was near an inlet and thus closer to the open ocean while the northern site (NS) was further from the ocean and closer to freshwater inputs. As a result, salinity tends to be higher at SS than NS (Chapman et al., 2021). Previous work at SS has also indicated that salinity can be very high during summer (up to 60 ppt) and lower during winter (48 ppt) (Dangremond et al., 2020). Previous studies have found small increases in *R* with increasing salinity, presumably due to costs associated with maintaining cellular ion gradients (Lopez-Hofmann et al., 2007; Aspinwall et al., 2021). Thus, the combination of warmer growth temperatures and higher salinity might explain why *R* increased with T_{air} at SS, and why temperature acclimation appeared constrained.

However, averaged across sites, *Avicennia* also increased respiratory capacity in response to experimental warming, suggesting that salinity alone is unlikely to explain the increase in *R* with warmer growth temperatures. Instead, coordination between *R* and photosynthetic capacity might explain the positive relationship between growth temperature and respiratory capacity in *Avicennia*. Importantly, we found that variation in respiratory capacity (e.g. R_{mass}^{25}) over time and across sites and treatments was largely explained by changes in leaf N concentrations. The coupling of leaf N and respiratory capacity could represent enzyme limitation of respiratory capacity (Ryan et al., 1996). However, leaf N and Rubisco carboxylation (V_{cmax}) show a general positive relationship across C_3 species given that a large fraction of N is allocated to Rubisco. A

new theory also indicates that temperature acclimation of R is consistent with maintenance of 'optimal' photosynthetic capacity, where respiratory capacity increases to support processes that maintain photosynthesis (Wang et al., 2020). We hypothesize that respiratory capacity increased with temperature in *Avicennia* due to concomitant changes in photosynthetic capacity, which were reflected in changes in leaf N. If true, *Avicennia* responded to increasing growth temperature by also increasing photosynthetic capacity; a response which is not necessarily consistent with studies of photosynthetic temperature acclimation over space and time (Way and Sage 2008; Way and Yamori 2014; Ali et al., 2015).

Temporal patterns in leaf R and leaf N in *Avicennia* may have also been influenced by nutrient availability, which could vary with air and soil temperature. Warmer soil and water temperatures during summer may speed up decomposition and N mineralization (Kirwan & Blum 2011; Gao et al., 2014) which could increase N availability and potentially result in higher leaf N concentrations. Results from a fertilization experiment near our southern site have demonstrated that higher N availability leads to higher leaf N concentrations in *Avicennia* (Simpson et al., 2013; Dangremond et al., 2020). Although seasonal changes in N availability were not quantified in our study, we found that leaf N concentrations increased in *Avicennia* with prevailing air temperature across both sites. Therefore, higher N availability during warmer time periods may have resulted in higher leaf N, greater photosynthetic capacity, and coordinated increases in respiratory capacity in *Avicennia* (Wang et al., 2020).

Although respiratory capacity increased with growth temperature in *Avicennia*, indicating no Type II temperature acclimation, we observed a decline in the short-term Q_{10} of R as prevailing T_{air} increased across seasons (i.e. Type I acclimation, Atkin & Tjoelker 2003; Slot & Kitajima, 2015). This acclimation response is less common but has been observed in several studies (Atkin et al., 2000; Zaragoza-Castells et al., 2007; Ow et al., 2010). Mechanisms of Type I acclimation are unclear although regulatory changes in respiratory enzymes could be involved (Atkin et al., 2005; Kruse et al., 2011; 2020). Other studies have identified positive relationships between soluble sugars and the Q_{10} of R (Azcón-Bieto et al., 1983; Ow et al., 2010) which could reflect substrate limitation of the maximum catalytic enzyme activity (Atkin & Tjoelker 2003). It is possible that high respiratory demand during summer may have reduced soluble sugar concentrations which in turn reduced maximum catalytic activity and the temperature sensitivity of R.

553 The complexity of C_4 photosynthesis has been hypothesized to come at a cost of reduced
554 phenotypic plasticity or lower temperature acclimation capacity in C_4 plants (Sage & McKown,
555 2006; Yamori et al., 2014). Yet, experimental work has found no clear differences in temperature
556 acclimation responses between C_3 and C_4 plant species (Smith & Dukes, 2017). We tested the
557 hypothesis that *Spartina* would show weaker temperature acclimation than *Avicennia* and found
558 no support for this expectation. In fact, we found that *Spartina* reduced R_{mass}^{25} and the short-term
559 Q_{10} of R as growth temperatures increased (Type II acclimation and Type I acclimation) over
560 time and across sites and treatments while *Avicennia* generally showed *increased* respiratory
561 capacity with temperature. The temperature acclimation results in *Spartina* are similar to results
562 from other studies with tree species representing different biomes (Aspinwall et al., 2016; Reich
563 et al., 2016). We conclude that *Spartina*, a dominant C_4 marsh grass, showed rather consistent
564 temperature acclimation of R over space and time, and with climate warming, which could
565 reduce the temperature sensitivity of CO_2 fluxes in marsh-dominated coastal wetlands.
566 Convergent temperature acclimation in *Spartina* could be partly influenced by the modest
567 warming created by our passive warming chambers. The chambers increased mean daily T_{air} 0.6
568 to 0.7 °C and maximum daily T_{air} ~3 °C. At the same sites, Chapman et al., (2021) found the
569 chambers increased mean daytime T_{air} 1.6 °C. For context, average T_{air} across the contiguous
570 U.S. has increased 0.7 °C since the 1960s, with additional warming of ~1.4 °C expected over the
571 next few decades (USGCRP, 2018). A similar amount of warming is expected in the southeast
572 U.S. (Ashfaq et al., 2016). Therefore, the warming created by the chambers is within the range of
573 warming expected over the next few decades. Moreover, warming increased respiratory capacity
574 of *Avicennia*, indicating that the warming treatment was sufficient to alter biological processes.
575 Local adaptation or temperature seasonality across the species range could have
576 contributed to differences in temperature acclimation between species. The location of our
577 experiment is near the southern (warm) limit of *Spartina* and the northern (cool) limit of
578 *Avicennia* on the Atlantic coast. Both species have shown evidence of local adaptation and may
579 possess traits that influence their acclimation capacity (Markley et al., 1982; Kirwan et al., 2009;
580 Cook-Patton et al., 2015; Kennedy et al., 2020; Osland et al., 2020). However, robust
581 temperature acclimation in *Spartina* might be explained by the relatively high temperature
582 seasonality across the species range. Weaker temperature acclimation in *Avicennia* might be
583 consistent with less temperature seasonality across the species range. Nonetheless, studies that

584 have compared acclimation responses among species from more- or less-seasonal climates have
585 found no clear differences (Reich et al., 2016; Scafaro et al., 2017). Additional studies would be
586 required to understand the potential influence of local adaptation or species climatic niche on
587 temperature acclimation responses in coastal plants.

588 Repeated measurements of the short-term temperature response of *R* provided a powerful
589 approach for examining the consequence of species differences in temperature acclimation.
590 Using individual temperature response measurements to estimate realized (*in situ*) *R*, we found
591 that the Q_{10} of realized *R* was similar to the short-term Q_{10} of *R* in *Avicennia*. In *Avicennia*, we
592 also found that the ratio describing the degree of respiratory homeostasis ($Acclim_{homeo}$) declined
593 quickly with larger increases in growth temperature indicating that Type I acclimation alone was
594 not sufficient to dampen the temperature sensitivity of realized *R* and resulted in reduced
595 homeostasis of *R*. In *Spartina*, the Q_{10} of realized *R* was lower than the short-term Q_{10}.
596 Moreover, $Acclim_{homeo}$ declined more slowly with larger increases in T_{air}, especially when
597 $Acclim_{homeo}$ was calculated using estimates of *in situ* R_{mass}. Thus, Type II and Type I acclimation
598 in *Spartina* resulted in greater homeostasis of *R*. Our results agree with the synthesis of Slot &
599 Kitajima, (2015), who found that Type II acclimation results in greater homeostasis of *R* than
600 Type I acclimation alone.

601 Although species differed in temperature acclimation of *R*, leaf N explained temporal and
602 spatial variation in respiratory capacity in both species. Species differences in leaf N and *R* over
603 time may be partly related to different nutrient acquisition or investment strategies. For instance,
604 *Avicennia* is an evergreen species and is known to be very responsive to N availability (Simpson
605 et al., 2013; Dangremond et al., 2020). In our study, *Avicennia* decreased LMA and increased
606 leaf N as seasonal temperatures increased. Some studies have shown that *Spartina* is also
607 responsive to nutrients (e.g. Mendelssohn, 1979), although responses are variable among
608 individual studies (e.g., Weaver & Armitage, 2020). However, *Spartina* exhibits a strong
609 seasonality to leaf development and leaf N concentrations; as seasonal temperatures increase
610 LMA increases and leaf N decreases. These distinct seasonal patterns could explain the
611 contrasting seasonal responses of respiratory capacity, but the close coupling of leaf N and *R* in
612 both species.

613 More broadly, our results indicate that leaf N may be useful predictor of foliar C fluxes in
614 dominant coastal wetland species, just as leaf N is used to estimate leaf *R* in land surface models

that predict terrestrial C fluxes over space and time (Atkin et al., 2015; Fisher et al., 2014; Lawrence et al., 2019). In fact, in our species and across our sites, leaf N explained more variation in leaf R than prevailing T_{air}. We note that coastal wetlands are not well-represented in land surface models due to gaps in our understanding of key processes and data limitations (Ward et al., 2020). The data presented here could improve representation and parameterization of CO_2 exchange between coastal vegetation and the atmosphere in large-scale models.

Our results indicate that patterns of respiratory temperature acclimation may differ between co-occurring coastal wetland species representing different functional types. Convergent acclimation responses may be expected in some but not all species. Although acclimation patterns may differ among species, leaf N may be a useful predictor of respiratory capacity, and ultimately respiratory C fluxes across a range of growth temperatures. The data presented here will be particularly useful for improving predictions of C fluxes from coastal wetlands under current and future climate conditions. Nonetheless, studies that examine coordination of leaf respiratory and photosynthetic capacity over temporal and spatial gradients will provide further insight into aboveground physiological controls of coastal wetland C cycling.

Acknowledgements

This work was funded by NSF DEB 1655659 awarded to SKC. Support for MJA and JC were provided by USDA-NIFA award 2019-67013-29161, the University of North Florida, and Auburn University. Additional support for MAS was provided by the Garden Club of America Award in Coastal Wetlands Studies. The authors thank GTMNERR staff and volunteers for their support and assistance with this experiment.

Author contributions

SKC, MAS, and MJA conceived and designed the experiment. MAS and GC collected data. MAS, JC, and MJA analyzed the data. MAS and MJA wrote the manuscript with input from all authors.

Data Sharing and Accessibility

All data used in this manuscript are publicly available and can be accessed at https://doi.org/10.5281/zenodo.5567749

646
647
648
649
650

651 **References**

652

653 Akaji, Y., Inoue, T., Tomimatsu H. & Kawanishi A. (2019) Photosynthesis, respiration, and
654 growth patterns of *Rhizophora stylosa* seedlings in relation to growth
655 temperature. *Trees* 33, 1041–1049.
656 Ali A.A., Xu C.G., Rogers A., McDowell N.G., Medlyn B.E., Fisher R.A., Wullschleger S.D.,
657 Reich P.B., Vrugt J.A., Bauerle W.L., Santiago L.S., & Wilson C.J. (2015) Global-scale
658 environmental control of plant photosynthetic capacity. *Ecological Applications* 25:
659 2349–2365.
660 Alongi, D.M. (2020) Carbon Balance in Salt Marsh and Mangrove Ecosystems: A Global
661 Synthesis. *Journal of Marine Science and Engineering* 8(10), 767.
662 Ashfaq M., Rastogi D., Mei R., Kao S-C., Grangrade S., Naz B. & Touma D. (2016) High-
663 resolution ensemble projections of near-term regional climate over the continental United
664 States. *Journal of Geophysical Research: Atmospheres* 121(17), 9943-9963.
665 Aspinwall, M. J., Drake, J. E., Campany, C., Vårhammar, A., Ghannoum, O., Tissue, D. T.,
666 Reich, P.B., & Tjoelker, M.G. (2016). Convergent acclimation of leaf photosynthesis and
667 respiration to prevailing ambient temperatures under current and warmer climates in
668 *Eucalyptus tereticornis*. *New Phytologist* 212, 354–367.
669 Aspinwall, M., Vårhammar, A., Blackman, C., Tjoelker, M., Ahrens, C., Byrne, M., Tissue,
670 D.T., & Rymer, P. (2017). Adaptation and acclimation both influence photosynthetic and
671 respiratory temperature responses in Corymbia calophylla. *Tree Physiology* 37(8), 1095–
672 1112.
673 Aspinwall, M. J., Pfautsch, S., Tjoelker, M. G., Vårhammar, A., Possell, M., Drake, J. E., Reich,
674 P. B., Tissue, D. T., Atkin, O. K., Rymer, P. D., & Dennison, S. (2019). Range size and
675 growth temperature influence Eucalyptus species responses to an experimental heatwave.
676 *Global Change Biology* 25, 1665–1684.
677 Aspinwall, M.J., Faciane, M., Harris, K., O'Toole, M., Neece, A., Jerome, V., Colón, M.,
678 Chieppa, J., & Feller I.C. (2021) Salinity has little effect on photosynthetic and
679 respiratory responses to seasonal temperature changes in black mangrove (*Avicennia*
680 *germinans*) seedlings. *Tree Physiology* 41(1) 103–118.
681 Atkin, O.K., Evans, J.R., Ball, M.C., Lambers, H., & Pons, T.L. (2000). Leaf respiration of snow

682 gum in the light and dark. Interactions between temperature and irradiance. *Plant*
683 *Physiology* 122, 915–923.
684 Atkin, O.K. & Tjoelker, M.G. (2003). Thermal acclimation and the dynamic response of plant
685 respiration to temperature. *Trends in plant science* 8, 343-351.
686 Atkin, O.K., Bruhn, D., Hurry, V.M., & Tjoelker, M.G. (2005). Evans Review No. 2:
687 The hot and the cold: unravelling the variable response of plant respiration to
688 temperature. *Functional Plant Biology* 32, 87-105.
689 Atkin, O. K., Scheurwater I., & Pons T.L. (2007). Respiration as a percentage of daily
690 photosynthesis in whole plants is homeostatic at moderate, but not high, growth
691 temperatures. *New Phytologist* 174, 367– 380.
692 Atkin, O.K., Meir P., & Turnbull M.H. (2014). Improving representation of leaf respiration in
693 large-scale predictive climate-vegetation models. *New Phytologist* 202(3), 743–748.
694 Atkin, O.K., Bloomfield, K.J., Reich, P.B., Tjoelker, M.G., Asner, G.P., Bonal, D., …. &
695 Zaragoza-Castells. J. (2015). Global variability in leaf respiration in relation to climate,
696 plant functional types and leaf traits. *New Phytologist* 206, 614-636
697 Azcón-Bieto, J., Lambers, H., & Day, D.A. (1983). Effect of photosynthesis and carbohydrate
698 status on respiratory rates and the involvement of the alternative pathway in leaf
699 respiration. *Plant Physiology* 72, 598–603.
700 Bolstad P.V., Reich P.B., & Lee T. (2003). Rapid temperature acclimation of leaf respiration
701 rates in *Quercus alba* and *Quercus rubra*. *Tree Physiology* 23(14), 969–976.
702 Bouillon S., Borges A.V., Castaneda-Moya E., Diele K., Dittmar T., Duke N.C., & Twilley R.R.
703 (2008). Mangrove production and carbon sinks: A revision of global budget estimates.
704 *Global Biogeochemical Cycles* 22(2).
705 Bruhn D., Egerton J.J.G., Loveys B.R., & Ball M.C. (2007). Evergreen leaf respiration
706 acclimates to long-term nocturnal warming under field conditions. *Global Change*
707 *Biology* 13, 1216–1223.
708 Chapman S.K., Feller I.C., Canas G., Hayes M.A., Dix N., Hester M., Morris J., & Langley J.A.
709 (2021). Mangrove growth response to experimental warming is greatest near the range
710 limit in northeast Florida. *Ecology* 10(6).
711 Cheesman A.W., & Winter K. (2013). Growth response and acclimation of CO_2 exchange

712 characteristics to elevated temperatures in tropical tree seedlings. *Journal of*
713 *Experimental Botany* 64, 3817– 3828.
714 Cook-Patton S.C., Lehmann M., & Parker J.D. (2015) Convergence of three mangrove species
715 towards freeze-tolerant phenotypes at an expanding range edge. *Functional Ecology*, 29,
716 1332-1340.
717 Crous K.Y., Wallin G., Atkin O.K., Uddling J., & af Ekenstam A. (2017). Acclimation of light
718 and dark respiration to experimental and seasonal warming are mediated by changes in
719 leaf nitrogen in *Eucalyptus globulus*. *Tree Physiology* 37(8),1069–1083.
720 Dangremond E.M., Simpson L.T., Osborne T.Z., & Feller I.C. (2020). Nitrogen Enrichment
721 Accelerates Mangrove Range Expansion in the Temperate–Tropical Ecotone. *Ecosystems*
722 23, 703–714.
723 De Boeck H.J., De Groote T. & Nijs I. (2012) Leaf temperatures in glasshouses and open-top
724 chambers. *New Phytologist* 194, 1155–1164.
725 Dix N., Brockmeyer R., Chapman S., Angelini C., Kidd S., Eastman S., & Radabaugh K.R.
726 (2021). Northeast Florida. In K.R. Radabaugh, C.E. Powell, R.P. Moyer (Eds.) Coastal
727 Habitat Integrated Mapping and Monitoring Program Report for the State of Florida.
728 Florida Fish and Wildlife Conservation Commission Fish and Wildlife Research Institute
729 Technical Report No. 21
730 Donato D., Kauffman J., Murdiyarso D., Kurnianto S., Stidham M. & Kanninen M. (2011).
731 Mangroves among the most carbon-rich forests in the tropics. *Nature Geoscience* 4, 293–
732 297.
733 Drake J.E., Aspinwall M.J., Pfautsch S., Rymer P.D., Reich P.B., Smith R.A., Crous K.Y.,
734 Tissue D.T., Ghannoum O., & Tjoelker M.G. (2015). The capacity to cope with climate
735 warming declines from temperate to tropical latitudes in two widely distributed
736 Eucalyptus species. *Global Change Biology* 21, 459–472.
737 Evans J.R. (1989) Photosynthesis and nitrogen relationships in leaves of C3 plants. *Oecologia*
738 78, 9–19.
739 Fisher J.B., Huntzinger D.N., Schwalm C.R., & Sitch S. (2014). Modeling the terrestrial
740 biosphere. *Annual Review of Environment and Resources* 39, 91–123.
741 Gallagher J. L. (1975). Effect of an ammonium pulse on the growth and elemental composition

of natural stands of *Spartina alterniflora* and *Juncus roemerianus*. *American Journal of Botany* 62, 644– 648.

Gao H., Bai J., He X., Zhao Q., Lu Q., & Wang J. (2014). High Temperature and Salinity Enhance Soil Nitrogen Mineralization in a Tidal Freshwater Marsh. *PLOS ONE* 9(4)

Ghannoum O., Evans J.R., Chow W.S., Andrews T.J., Conroy J.P., & von Caemmerer S. (2005). Faster Rubisco is the key to superior nitrogen-use efficiency in NADP-malic enzyme relative to NAD-malic enzyme C_4 grasses. *Plant Physiology* 137, 638–650.

Heskel M.A., O'Sullivan O.S., Reich P.B., Tjoelker M.G., Weerasinghe L.K., Penillard A., Egerton J.J.G., Creek D., Bloomfield K.J., Xiang J., Sinca F., Stangl Z.R., Torre A.M., Griffin K.L., Huntingford C., Hurry V., Meir P., Turnbull M.H., & Atkin O.K. (2016). Convergence in the temperature response of leaf respiration across biomes and plant functional types. *Proceedings of the National Academy of Sciences of the United States of America* 113(14), 3832– 3837.

Hikosaka K., & Shigeno A. (2009). The role of Rubisco and cell walls in the interspecific variation in photosynthetic capacity. *Oecologia* 160, 443–451.

Kennedy J.P., Preziosi R.F., Rowntree J.K., & Feller I.C. (2020). Is the central-marginal hypothesis a general rule? Evidence from three distributions of an expanding mangrove species, *Avicennia germinans* (L.) L. *Molecular Ecology*, 29, 704-719.

King A.W., Gunderson C.A., Post W.M., Weston D.J., & Wullschleger S.D. (2006). Plant respiration in a warmer world. *Science* 312, 536–537.

Kirwan M. L., Guntenspergen G.R., & Morris J.T. (2009). Latitudinal trends in *Spartina alterniflora* productivity and the response of coastal marshes to global change. *Global Change Biology* 15(8), 1982–1989.

Kirwan M.L. & Blum L.K. (2011). Enhanced decomposition offsets enhanced productivity and soil carbon accumulation in coastal wetlands responding to climate change. *Biogeosciences* 8, 987–993.

Kruse J., Rennenberg H., & Adams M.A. (2011). Steps towards a mechanistic understanding of respiratory temperature responses. *New Phytologist* 189, 659–677.

Kruse J., Turnbull T., Rennenberg H., & Adams M.A. (2020). Plasticity of Leaf Respiratory and Photosynthetic Traits in *Eucalyptus grandis* and *E. regnans* Grown Under Variable Light and Nitrogen Availability. *Frontiers in Forests and Global Change*.

773 Lawrence D. M., Fisher, R.A., Koven, C.D., Oleson, K.W., Swenson, S.C., Bonan, G., ….
774 Zeng X. (2019). The community land model version 5: Description of new features,
775 benchmarking, and impact of forcing uncertainty. *Journal of Advances in Modeling Earth*
776 *Systems* 11, 4245–4287.
777 Lee T. D., Reich P.B., & Bolstad P.V. (2005). Acclimation of leaf respiration to temperature is
778 rapid and related to specific leaf area, soluble sugars and leaf nitrogen across three
779 temperate deciduous tree species. *Functional Ecology* 19, 640–647.
780 Lloyd J., & Taylor J. (1994). On the Temperature Dependence of Soil Respiration. *Functional*
781 *Ecology* 8(3), 315-323.
782 Lombardozzi D., Bonan G., Smith N.G., Dukes J.S., & Fisher R. (2015). Temperature
783 acclimation of photosynthesis and respiration: a key uncertainty in the carbon cycle–
784 climate feedback. *Geophysical Research Letters* 42, 8624–8631.
785 Lopez-Hoffman L., Anten N.P.R., Martinez-Ramos M., & Ackerly D.D. (2007). Salinity and
786 light interactively affect neotropical mangrove seedlings at the leaf and whole plant
787 levels. *Oecologia* 150, 545–556.
788 Lu W., Xiao J., Liu F., Zhang Y., Liu C., & Lin G. (2017). Contrasting ecosystem CO_2 fluxes of
789 inland and coastal wetlands: a meta-analysis of eddy covariance data. *Global Change*
790 *Biology* 23(3), 1180-1198.
791 Lugo A.E., & Snedaker S.C. (1974). The ecology of mangroves. *Annual Review of Ecology and*
792 *Systematics* 5, 39–64.
793 Lugo A.E., Brown S.L., Dodson R., Smith T.S., & Shugart H.H. (1999). The Holdridge life
794 zones of the conterminous United States in relation to ecosystem mapping. *Journal of*
795 *Biogeography* 26, 1025-1038.
796 Markley, C. McMillan, G.A., & Thompson Jr. (1982). Latitudinal differentiation in response to
797 chilling temperatures among populations of three mangroves, *Avicennia germinans*,
798 *Laguncularia racemosa*, and *Rhizophora mangle*, from the western tropical Atlantic and
799 Pacific Panama. *Canadian Journal of Botany* 60, 2704-2715.
800 Mcleod E., Chmura G.L., Bouillon S., Salm R., Björk M., Duarte C.M., Lovelock
801 C.E., Schlesinger W.H., & Silliman B.R. (2011). A blueprint for blue carbon: Toward an
802 improved understanding of the role of vegetated coastal habitats in sequestering
803 CO_2. *Frontiers in Ecology and the Environment*, 9(10), 552-560.

804 Mendelssohn I.A. (1979). The influence of nitrogen level, form, and application method on the
805 growth response of *Spartina alterniflora* in North Carolina. *Estuaries* 2, 106– 112.
806 NOAA. National Climate Data Center website, https://www.ncdc.noaa.gov/cdo-web/webservices
807 , accessed on 4/2/20.
808 O'Leary B.M., Asao S., Millar A.H., & Atkin O.K. (2019). Core principles which explain
809 variation in respiration across biological scales. *New Phytologist* 222(2), 670– 686.
810 O'Sullivan O.S., Weerasinghe K.W., Evans J.R., Egerton J.J., Tjoelker M.G., & Atkin O.K.
811 (2013) High-resolution temperature responses of leaf respiration in snow gum
812 (*Eucalyptus pauciflora*) reveal high-temperature limits to respiratory function. *Plant, Cell*
813 *& Environment* 36, 1268–1284.
814 O'Sullivan O. S., Heskel M.A., Reich P.B., Tjoelker M.G., Weerasinghe L.K., Penillard A., ….
815 & Atkin O.K. (2017). Thermal limits of leaf metabolism across biomes. *Global Change*
816 *Biology* 23, 209–223.
817 Osland M.J., Day R.H., Hall C.T., Feher L.C., Armitage A.R., Cebrian J., …. & Synder C.M.
818 (2020) Temperature thresholds for black mangrove (*Avicennia germinans*) freeze
819 damage, mortality and recovery in North America: refining tipping points for range
820 expansion in a warming climate. *Journal of Ecology*, 108, 654-665.
821 Ow L.F., Whitehead D., Walcroft A.S., & Turnbull M.H. (2008). Thermal acclimation of
822 respiration but not photosynthesis in *Pinus radiata*. *Functional Plant Biology* 35, 448–
823 461.
824 Ow L.F., Whitehead D., Walcroft A.S., & Turnbull M.H. (2010). Seasonal variation in foliar
825 carbon exchange in *Pinus radiata* and *Populus deltoides*: respiration acclimates fully to
826 changes in temperature but photosynthesis does not. *Global Change Biology* 16, 288–
827 302.
828 Patterson A.E., Arkebauer R., Quallo C., Heskel M.A., Li X., Boelman N., & Griffin K.L.
829 (2018). Temperature response of respiration and respiratory quotients of 16 co-occurring
830 temperate tree species. *Tree Physiology* 38, 1319-1332.
831 Piao S.L., Sitch S., Ciais P., Friedlingstein P., Peylin P., Wang X.H., ….& Zeng N. (2013).
832 Evaluation of terrestrial carbon cycle models for their response to climate variability and
833 to CO_2 trends. *Global Change Biology* 19, 2117-2132.
834 R Core Team. (2013). R: a language and environment for statistical computing. Vienna, Austria:

R Foundation for Statistical Computing.

Reich P.B., Tjoelker M.G., Pregitzer K.S., Wright I.J., Oleksyn J., & Machado J.L. (2008). Scaling of respiration to nitrogen in leaves, stems and roots of higher land plants. *Ecology Letters* 11, 793-801.

Reich P. B., Sendall K. M., Stefanski A., Wei X., Rich R. L., & Montgomery R.A. (2016). Boreal and temperate trees show strong acclimation of respiration to warming. *Nature* 531, 633– 636.

Ryan M.G. (1991). Effects of climate change on plant respiration. *Ecological Applications* 1(2), 157–167.

Ryan M.G., Hubbard R.M., Pongracic S., Raison R.J., & McMurtrie R.E. (1996). Foliage, fine-root, woody-tissue and stand respiration in *Pinus radiata* in relation to nitrogen status. *Tree Physiology* 16(3), 333–343.

Sage R.F., & McKown A.D. (2006). Is C_4 photosynthesis less phenotypically plastic than C_3 photosynthesis? *Journal of Experimental Botany* 57, 303–317.

Scafaro A.P., Xiang S., Long B.M., Bahar N.H.A., Weerasinghe L.K., Creek D., Evans J.R., Reich P.B., Atkin O.K. (2017). Strong thermal acclimation of photosynthesis in tropical and temperate wet-forest tree species: the importance of altered Rubisco content. Global Change Biology, 23, 2783-2800.

Simpson L.T., Feller I.C., & Chapman S.K. (2013). Effects of competition and nutrient enrichment on *Avicennia germinans* in the salt marsh-mangrove ecotone. *Aquatic Botany* 104, 55–59.

Slot M., & Kitajima K. (2015). General patterns of acclimation of leaf respiration to warmer temperatures across biomes and plant types. *Oecologia* 177, 885–900.

Smith N.G., & Dukes J.S. (2013). Plant respiration and photosynthesis in global-scale models: incorporating acclimation to temperature and CO_2. *Global Change Biology* 19, 45-63.

Smith N.G., Malyshev S., Shevliakova E., Kattge J., & Dukes J.S. (2016). Foliar temperature acclimation reduces simulated carbon sensitivity to climate. *Nature Climate Change* 6, 407–411.

Smith N.G., & Dukes J.S. (2017). Short-term acclimation to warmer temperatures accelerates leaf carbon exchange processes across plant types. *Global Change Biology* 23, 4840–4853.

Smith N.G., McNellis R., & Dukes J.S. (2020). No acclimation: instantaneous responses to temperature maintain homeostatic photosynthetic rates under experimental warming across a precipitation gradient in *Ulmus americana*. *Annals of Botany- Plants* 12(4).

Tjoelker M.G., Oleksyn J., & Reich P.B. (1999). Acclimation of respiration to temperature and CO_2 in seedlings of boreal tree species in relation to plant size and relative growth rate. *Global Change Biology* 5, 679-691.

Tjoelker M.G., Oleksyn J., Reich P.B., & Zytkowiak R. (2008). Coupling of respiration, nitrogen, and Sugars underlies convergent temperature acclimation in *Pinus banksiana* across wide-ranging sites and populations. *Global Change Biology* 14, 782–797.

Tjoelker M.G., Oleksyn J., Lorenc-Plucinska G., & Reich P.B. (2009). Acclimation of respiratory temperature responses in northern and southern populations of Pinus banksiana. *New Phytologist* 181, 218–229.

USGCRP. (2018). Impacts, Risks, and Adaptation in the United States: Fourth National Climate Assessment, Volume II. [Reidmiller D.R., Avery C.W., Easterling D.R., Kunkel K.E., Lewis K.L.M., Maycock T.K., & Stewart B.C. (eds.)] U.S. Global Change Research Program. Washington, DC, USA. 1515 pp.

Vanderwel M. C., Slot M., Lichstein J.W., Reich P.B., Kattge J., Atkin O.K., Bloomfield K.J., Tjoelker M.G., & Kitajima K. (2015). Global convergence in leaf respiration from estimates of thermal acclimation across time and space. *New Phytologist* 207, 1026–1037.

Walker A.P., Beckerman A.P., Gu L., Kattge J., Cernusak L.A., Domingues T.F., ….& Woodward F.I. (2014). The relationship of leaf photosynthetic traits – Vc_{max} and J_{max} – to leaf nitrogen, leaf phosphorus, and specific leaf area: a meta-analysis and modeling study. *Ecology and Evolution* 4, 3218–3235.

Wang H., Atkin O.K., Keenan T.F., Smith N.G., Wright I.J., Bloomfield K.J., & Prentice I.C. (2020). Acclimation of leaf respiration consistent with optimal photosynthetic capacity. *Global Change Biology* 26(4), 2573–2583.

Ward N.D., Megonigal, J.P., Bond-Lamberty, B., Bailey, V.L., Butman, D., Canuel, E.A., …. & Windham-Myers, L. (2020). Representing the function and sensitivity of coastal interfaces in earth system models. *Nature Communications* 11(1), 2458.

Way D.A., & Sage R.F. (2008). Thermal acclimation of photosynthesis in black spruce (*Picea mariana* (Mill.) B.S.P.). *Plant, Cell and Environment* 31, 1250-1262.

Way D.A., & Yamori W. (2014). Thermal acclimation of photosynthesis: on the importance of adjusting our definitions and accounting for thermal acclimation of respiration. *Photosynthesis Research* 119, 89–100.

Weaver C. A., & Armitage A.R. (2020). Above- and belowground responses to nutrient enrichment within a marsh-mangrove ecotone. *Estuarine, Coastal and Shelf Science* 243:106884.

Wright I.J., Reich P.B., Westoby M., Ackerly D.D., Baruch Z., Bongers F., … & Villar R. (2004). The worldwide leaf economics spectrum. *Nature* 428, 821– 827.

Yamori W., Hikosaka K. & Way D.A. (2014). Temperature response of photosynthesis in C_3, C_4, and CAM plants: temperature acclimation and temperature adaptation. *Photosynthesis Research* 119, 101–117.

Zaragoza-Castells J., Sanchez-Gomez D., Valladares F., Hurry V., & Atkin O.K. (2007) Does growth irradiance affect temperature dependence and thermal acclimation of leaf respiration? Insights from a Mediterranean tree with long-lived leaves. *Plant, Cell and Environment* 30, 820-833.

925 **Table 1.** Results of a three-way analysis of variance testing the main and interactive effects of temperature treatment (T),
926 measurement date (D), and site (S) on rates of leaf dark respiration per unit area and per unit mass at 25 °C (R_{area}^{25}, R_{mass}^{25}), the
927 temperature sensitivity of *R* estimated at 25 °C (Q_{10}^{25}), leaf dry mass per unit area (LMA), and leaf nitrogen on per unit area and per
928 unit mass (N_{mass}, N_{area}) in *Spartina alterniflora* and *Avicennia germinans*. Degrees of freedom (*df*) and *F*-values are presented for each
929 factor and reponse variable. *F*-values with '*', '**' and '***' are significant at $P<0.05$, $P<0.01$, and $P<0.001$, respectively.
930

		Treatment (T)		Date (D)		Site (S)		T × D		T × S		D × S		T × D × S	
Species	Trait	*df*	*F*	*df*	*F*	*df*	*F*	*df*	*F*	*df*	*F*	*df*	*F*	*df*	*F*
Avicennia germinans	R_{area}^{25}	1	9.05**	5	10.00***	1	0.50	5	0.35	1	1.92	5	5.96***	5	0.48
	R_{mass}^{25}	1	6.79*	5	10.09***	1	9.38**	5	0.34	1	5.27*	5	7.57***	5	0.86
	Q_{10}^{25}	1	0.39	5	9.88***	1	19.38***	5	0.63	1	0.57	5	1.39	5	0.32
	LMA	1	1.95	5	13.29***	1	32.77***	5	0.83	1	6.18*	5	3.87**	5	2.41*
	N_{mass}	1	0.83	2	3.34*	1	0.44	2	0.14	1	0.20	2	0.57	2	0.42
	N_{area}	1	0.05	2	0.08	1	9.18**	2	1.34	1	3.46	2	3.69*	2	0.09
Spartina alterniflora	R_{area}^{25}	1	1.75	5	3.17*	1	0.69	5	0.58	1	0.42	5	2.33*	5	0.49
	R_{mass}^{25}	1	4.83*	5	15.67***	1	12.03***	5	0.51	1	2.68	5	3.53**	5	0.22
	Q_{10}^{25}	1	2.76	5	4.62***	1	0.62	5	0.73	1	2.43	5	0.82	5	0.66
	LMA	1	0.04	5	22.57***	1	2.88	5	0.54	1	0.42	5	4.29**	5	0.37
	N_{mass}	1	0.41	2	15.32***	1	1.82	2	5.55**	1	0.01	2	0.86	2	0.43
	N_{area}	1	0.02	2	2.03	1	1.23	2	2.20	1	0.42	2	1.68	2	0.21

931
932
933
934

935
936
937
938
939
940

941 **Table 2.** Analysis of covariance results (*F*-values) testing the relationship between mean daily air temperature (T_{air}) of the preceding 7
942 days and leaf traits for *Spartina alterniflora* and *Avicennia germinans* and the influence of site and temperature treatment. *F*-values
943 with '*', '**' and '***' are significant at $P<0.05$, $P<0.01$, and $P<0.001$, respectively.
944

Species	Source of variance	R_{area}^{25}	R_{mass}^{25}	Q_{10}^{25}	LMA	N_{mass}	N_{area}
Avicennia germinans	T_{air}	6.23*	26.38***	20.81***	44.62***	5.80*	0.16
	Treatment (T)	6.85**	4.94*	0.13	0.98	0.76	0.12
	Site (S)	0.24	6.90**	23.80***	23.26***	0.42	9.04**
	T_{air} × T	0.72	0.04	0.14	0.19	0.50	2.84
	T_{air} × S	18.19***	25.24***	0.64	12.08***	0.34	0.03
	T × S	1.44	3.89	0.22	4.62*	0.23	2.84
	T_{air} × T × S	0.23	0.76	0.35	2.10	0.16	0.01
Spartina alterniflora	T_{air}	1.07	86.88***	14.52***	59.77***	34.93***	0.63
	Treatment (T)	1.59	3.02	2.17	0.08	0.06	0.01
	Site (S)	0.39	6.18*	1.51	0.51	2.11	1.05
	T_{air} × T	1.06	3.23	2.38	0.05	12.74***	3.65
	T_{air} × S	0.36	2.98	1.69	3.17	0.42	3.31
	T × S	0.11	1.71	1.75	0.43	0.01	0.59
	T_{air} × T × S	1.24	0.31	1.06	0.50	0.37	0.95

945
946 Variable descriptions: R_{area}^{25}, leaf respiration per unit area at 25 °C; R_{mass}^{25}, leaf respiration per unit mass at 25 °C; Q_{10}^{25}, the
947 temperature sensitivity of leaf *R* at 25 °C; LMA, leaf mass per unit area; N_{area}, leaf N per unit area; N_{mass}, leaf N per unit mass.

948
949
950
951
952
953
954
955

956 **Table 3.** Analysis of covariance results (*F*-values) testing relationships between leaf nitrogen
957 concentrations (area- and mass-basis; N_{area}, N_{mass}) and leaf respiration at 25 °C (area- and mass-
958 basis, R_{area}^{25}, R_{mass}^{25}) in *Avicennia germinans* and *Spartina alterniflora*. *F*-values with '*', '**'
959 and '***' are significant at $P<0.05$, $P<0.01$, and $P<0.001$, respectively.
960

Response variable = R_{area}^{25}		
Source of variance	*Avicennia germinans*	*Spartina alterniflora*
N_{area}	5.77*	154.20***
Treatment (T)	4.18*	2.59
Site (S)	0.17	0.00
N_{area} × T	0.02	0.21
N_{area} × S	7.54**	5.41*
T × S	1.37	2.06
N_{area} × T × S	0.30	0.20
Response variable = R_{mass}^{25}		
Source of variance	*Avicennia germinans*	*Spartina alterniflora*
N_{mass}	50.73***	51.25***
Treatment (T)	3.47	3.10
Site (S)	4.51*	0.82
N_{mass} × T	0.36	0.03
N_{mass} × S	3.24	0.82
T × S	3.47	3.46
N_{mass} × T × S	0.63	0.41

961
962
963
964
965
966
967

968
969
970
971
972
973
974
975
976
977
978
979
980

981 **Figure captions**

982

983 **Figure. 1.** Mean values (± standard error, $n = 6$) for several leaf traits over time in *Avicennia*
984 *germinans* and *Spartina alterniflora* growing at two sites in North Florida (North, South) under
985 two temperature treatments (Ambient, Warmed). Variable descriptions: R_{area}^{25}, leaf respiration
986 per unit area at 25 °C (panels a, b); R_{mass}^{25}, leaf respiration per unit mass at 25 °C (panels c, d);
987 Q_{10}^{25}, the temperature sensitivity of R estimated at 25 °C (panels e, f); LMA, leaf mass per unit
988 area (panels g, h); N_{area}, leaf N per unit area (panels i, j); N_{mass}, leaf N per unit mass (panels k, l).

989

990 **Figure. 2.** The relationship between thermal history (mean daily air temperature (T_{air}) of
991 preceding 7 days) and leaf physiological traits for *Avicennia germinans* and *Spartina alterniflora*
992 growing at two sites in North Florida (North, South) under two temperature treatments (Ambient,
993 Warmed). Variable descriptions: R_{area}^{25}, leaf respiration per unit area at 25 °C (panels a, b);
994 R_{mass}^{25}, leaf respiration per unit mass at 25 °C (panels c, d); Q_{10}^{25}, the temperature sensitivity of
995 R estimated at 25 °C (panels e, f); LMA, leaf mass per unit area (panels g, h); N_{area}, leaf N per
996 unit area (panels i, j); N_{mass}, leaf N per unit mass (panels k, l). Gray solid lines signify a common
997 relationship across sites and treatments. Black solid and dashed lines signify different
998 relationships between sites. Red and blue lines signify different relationships between treatments

that are consistent across sites. Intercept and slope parameters for the relationships are provided in Table S3).

Figure. 3. The (long-term) response of *in situ* rates of leaf *R* (area- and mass-basis, R_{area}, R_{mass}) to prevailing mean daily air temperature (T_{air}) in *Avicennia germinans* and *Spartina alterniflora* growing at two sites in North Florida (North, South) under two temperature treatments (Ambient, Warmed). An exponential function that estimates the Q_{10} of *R* and *R* at a reference temperature of 18 °C (R_{18}) was fit to the data. For each species, we compared Q_{10} estimates and R_{18} between sites and treatments by calculating 95% confidence intervals (standard error × 1.96) of the parameter estimates. When confidence intervals for Q_{10} and R_{18} did not overlap between sites or treatments, we fit separate temperature response functions for each site (solid and dashed lines) or treatment (blue and red lines). If confidence intervals of parameter estimates overlapped, suggesting that parameters were not different between sites or treatments, we fit a single temperature response function across all data (grey lines).

Figure. 4. The relationship between the ratio describing the degree of respiratory homeostasis over time ($Acclim_{homeo}$ = *R* at lowest mean daily T_{air} / *R* at mean daily T_{air}) and the degree of seasonal temperature change (ΔT_{air} = mean daily T_{air} – lowest mean daily T_{air}) for *Avicennia germinans* and *Spartina alterniflora* growing at two sites in North Florida (North, South) under two temperature treatments (blue = Ambient, red = Warmed). $Acclim_{homeo}$ ratios > 1 indicate temperature acclimation resulting in overcompensation (*R* at high T_{air} > *R* at low T_{air}), ratios = 1 indicate temperature acclimation resulting in complete homeostasis, and ratios < 1 indicate temperature acclimation resulting in partial homeostasis. Ratios are shown on an area basis (panels a,b) and mass basis (panels c,d). When the intercept or slope of the relationship between $Acclim_{homeo}$ and ΔT_{air} differed between sites, we fit separate lines for each site (solid versus dashed line). Within each panel, the extent to which ΔT_{air}, site, treatment, or their interactions explained variation in $Acclim_{homeo}$ is denoted by asterisks: *, $p<0.05$; **, $p<0.01$; ***, $p<0.001$.

Figure. 5. The relationship between leaf N concentrations (area- and mass-basis; N_{area}, N_{mass}) and leaf respiration at 25 °C (area- and mass-basis; R_{area}^{25}, R_{mass}^{25}) in *Avicennia germinans* (panels a, c) and *Spartina alterniflora* growing at two sites in North Florida (North, South) under two

temperature treatments (blue = Ambient, red = Warmed). Gray solid lines signify a common relationship across sites and treatments. Black solid and dashed lines signify different relationships between sites. Red and blue lines signify different relationships between treatments that are consistent across sites. Intercept and slope parameters and model coefficients of variation (R^2) are provided in Table S4.

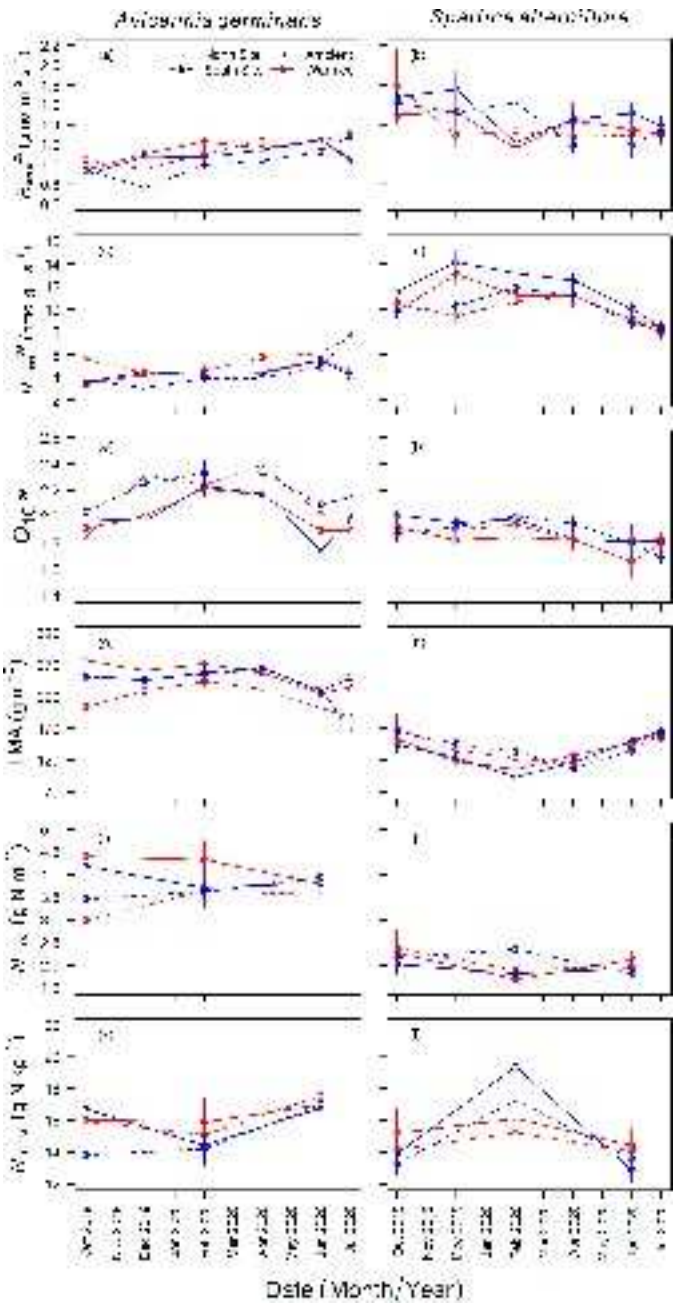

gcb_15938_f1.tiff

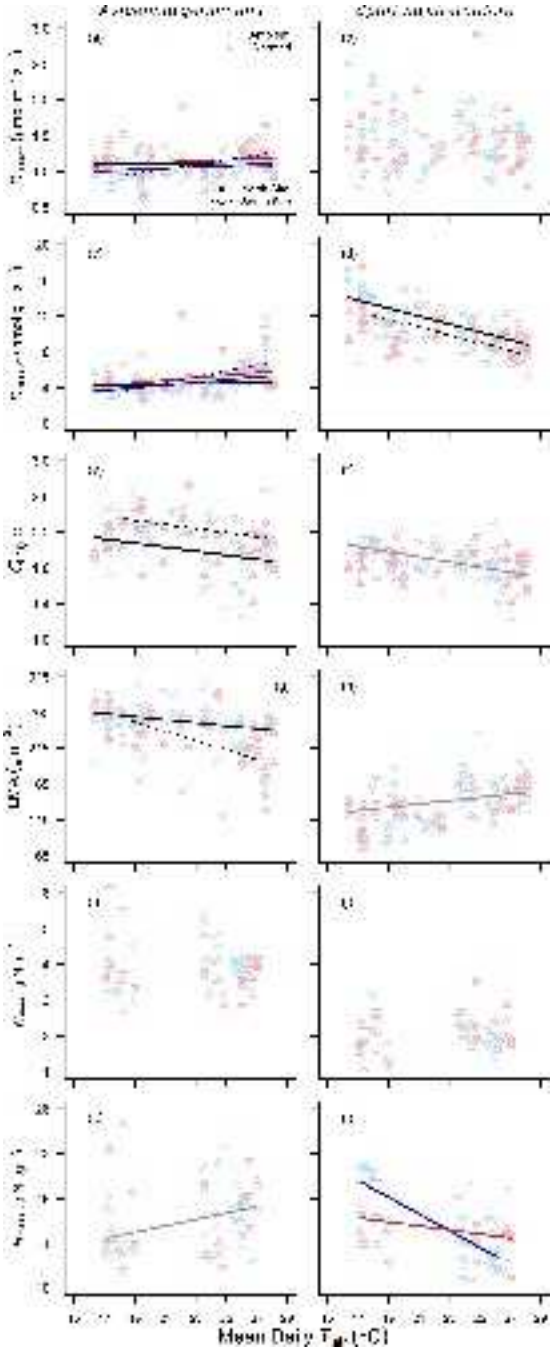

gcb_15938_f2.tiff

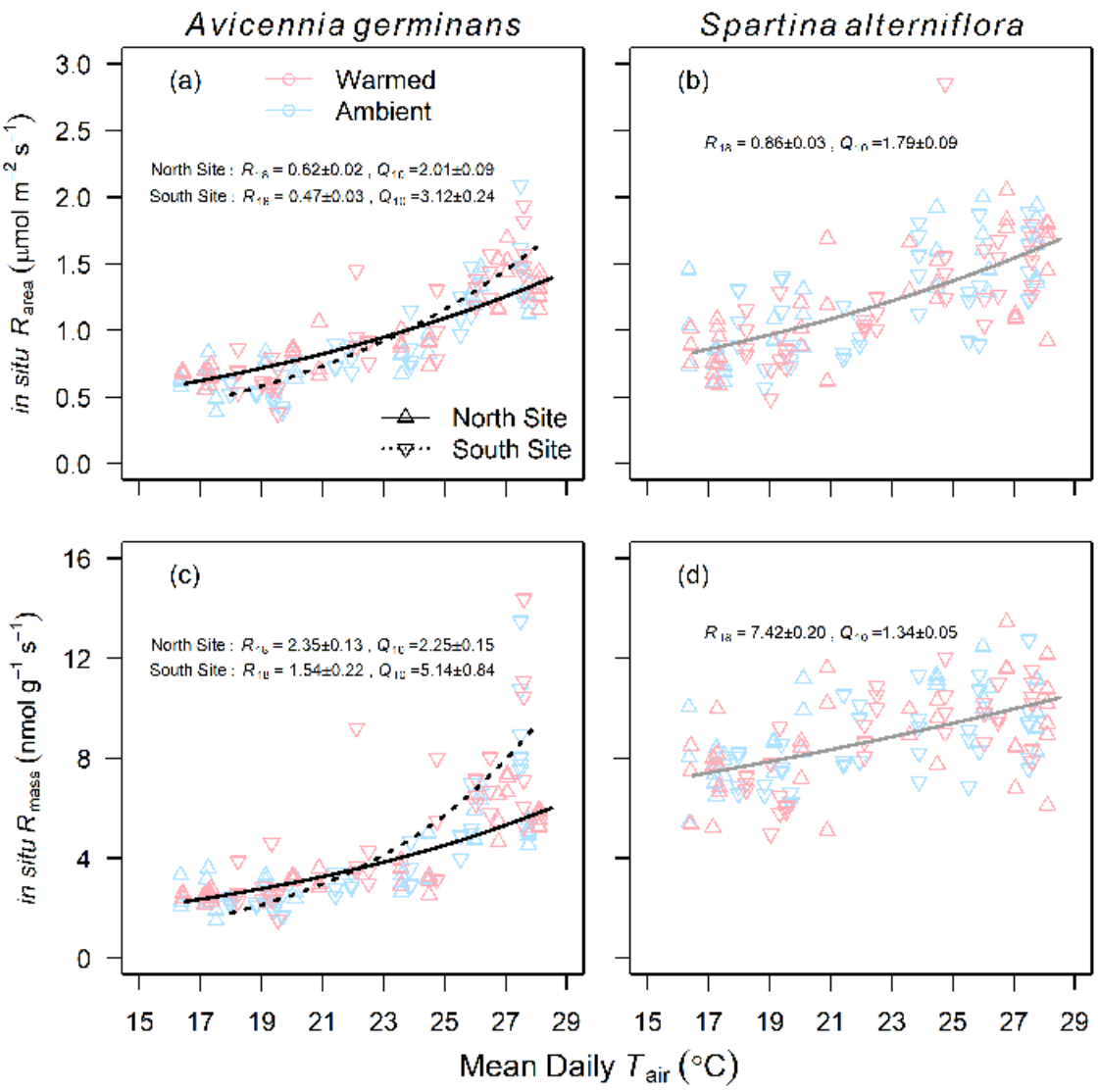

gcb_15938_f3.tiff

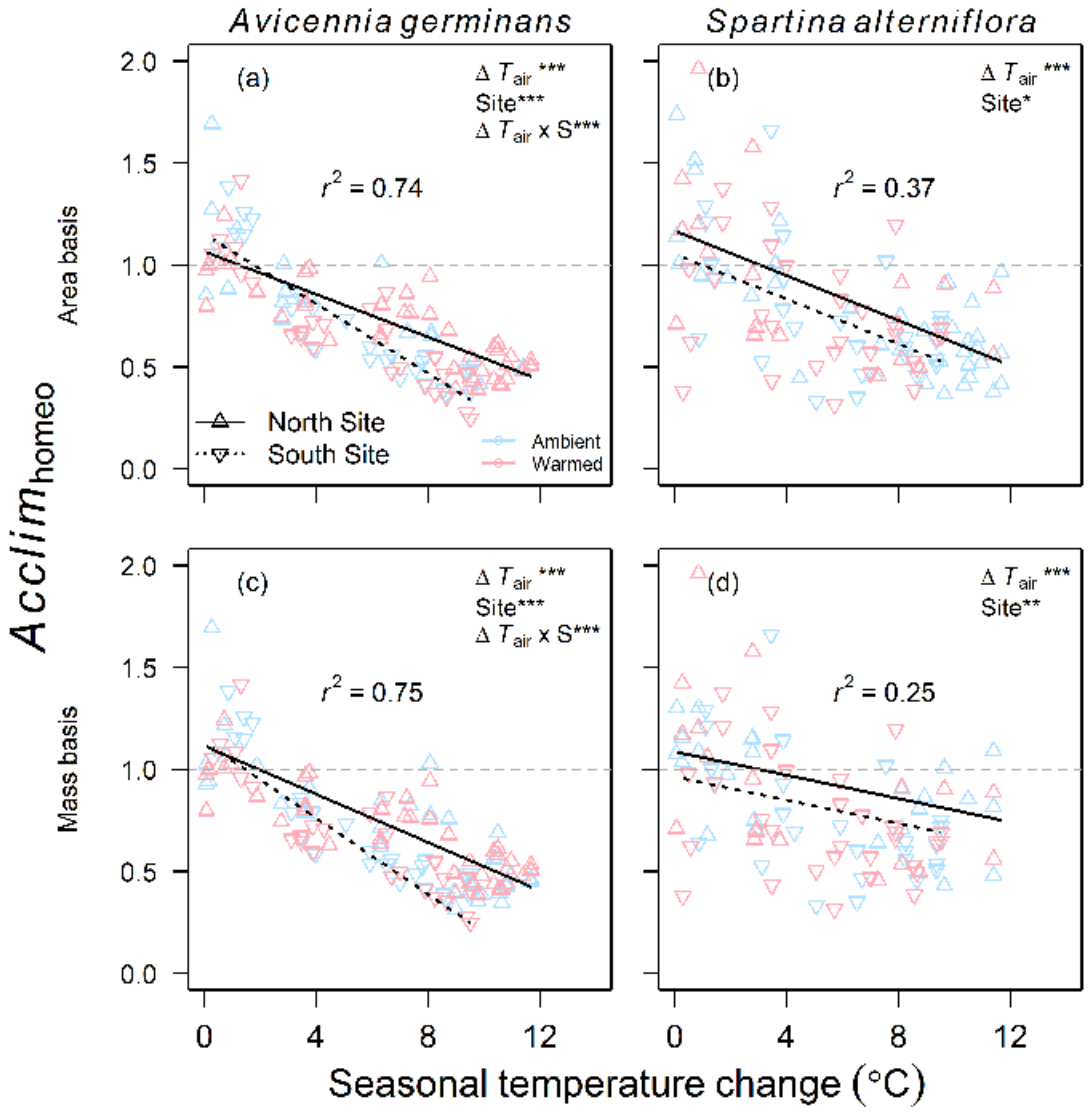

gcb_15938_f4.tiff

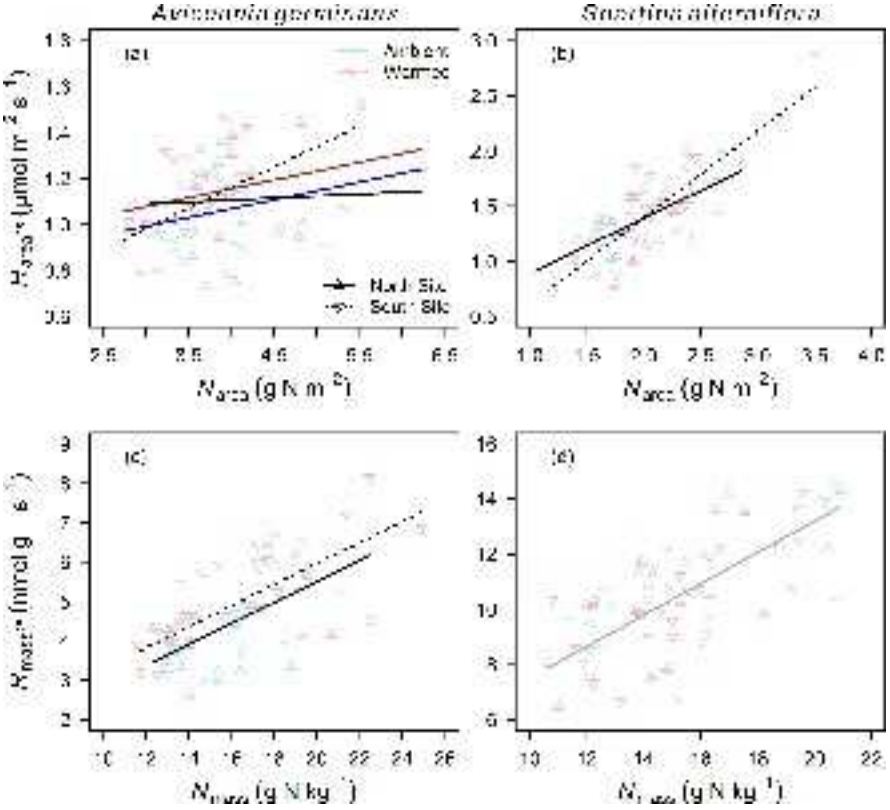

gcb_15938_f5.tiff